Linear Parameter Varying Control for XV-15 Tiltrotor Vehicle during Transition

Hao Yang
School of Engineering
University of Leicester
Email: hy153@le.ac.uk

Rafael M. Morales
School of Engineering
University of Leicester
Email: rmm23@le.ac.uk

Abstract

This manuscript applies Linear-Parameter-Varying control methods to a validated XV-15 tilt rotor vehicle, aiming to develop the flight control system specifically for the transition period. The proposed control law uses self-scheduling $\mathcal{H}_\infty$ design synthesis, which not only guarantees the closed-loop stability over the entire parameter space, but also ensures a prescribed level of performance. Simulation results show that the controller can offer very good performance in terms of reference tracking and disturbance rejection, indicating that the pilot's workload can be reduced significantly.

Nomenclature

$u/v/w$	forward/lateral/vertical velocity perturbation [kt]
$\phi/\theta/\psi$	roll/pitch/yaw attitude perturbation [deg]
$p/q/r$	roll/pitch/yaw rate perturbation [deg/s]
$\theta_{0,C}$	common collective pitch [deg]
$\theta_{0,D}$	differential collective pitch [deg]
$\theta_{1s,C}$	common longitudinal cyclic [deg]
$\theta_{1s,D}$	differential longitudinal cyclic [deg]
$\delta_a/\delta_e/\delta_r$	aileron/elevator/rudder deflection [deg]
$\theta_{lon,c}/\theta_{lat,c}/\theta_{y,c}$	combined longitudinal/lateral/yawing controller [inch]
β_m	nacelle incidence [deg]
V_0	flight speed [kt]

I. Introduction

Tilt rotor vehicles are able to perform vertical taking-off/landing (VTOL) as well as high speed forward flight, for this reason, this type of aircraft has attracted numerous interests. In general, three main configurations can be identified for such aircraft: i) helicopter, in which the flight control system uses swashplate inputs; ii) fixed wing, where standard flight control surfaces are used iii) transition, in which the flight control is typically delivered by using both swashplate and flight control surface inputs. Among these three modes, the transition is regarded as the most crucial one since the vehicle's aerodynamics undergoes significant changes when it converts from one configuration to another. As a result, the workload of the pilot during such period is high, not only because of the complex flight dynamics, but also due to the control couplings between the swashplate inputs and the flight control surfaces.

To the authors' best knowledge, although various control methods, such as $\mathcal{H}_\infty$ [1]–[3], Proportional-Integral-Derivative (PID) [4]–[6], Linear-Parameter-Varying (LPV) [7]–[9] and Nonlinear-Dynamic-Inversion (NDI) [10], [11], have been explored on tilt rotor vehicles, most of them are used for the development of helicopter and fixed wing controllers. On the other hand, the flight control for transition is typically delivered by using gain scheduling between the helicopter and fixed wing controller [8], [12], [13], i.e., as the nacelle incidence tilts forward, the swashplate inputs are gradually phased out and the flight control surface inputs become dominant. However, such scheduling can be unreliable in practice since it provides no stability guarantee for the closed-loop, and the scheduling algorithm needs to be carefully tuned.

Motivated by the afore-mentioned limitations, this work aims to develop flight control system dedicated for the transition period, where a Linear-Matrix-Inequalities (LMIs) based LPV design synthesis, known as self-scheduling $\mathcal{H}_\infty$ control [19]–[22], is exploited. By solving a set of optimisation problems, a LPV controller stabilising the closed-loop over the entire parameter space can be obtained, which also ensures that the worst-scenario performance level is bounded by a prescribed value. The application of LPV control to aerospace

applications can be traced back decades ago, see for instance [16]–[18], and it fits explicitly well for the applications where the system dynamics experiences large variations, such as the control problem stated in this work. Compared with Linear-Time-Invariant (LTI) control methods such as PID and $\mathcal{H}_\infty$, the LPV methods can offer better control results and guarantee similar performance level over the considered flight envelope.

This manuscript is structured into 5 sections. Section 2 introduces the self-scheduling $\mathcal{H}_\infty$ control approach, which is used for the flight control system design in Section 3. Section 4 presents the simulation results, which are performed on linearised models. This paper concludes with some final remarks in Section 5.

II. Self-scheduling $\mathcal{H}_\infty$ Control

The self-scheduling $\mathcal{H}_\infty$ control tackles a quadratic $\mathcal{H}_\infty$ γ-performance problem defined in Fig. 1, where the LPV system $\mathbf{P}(\boldsymbol{\rho})$ is called the generalised plant, whose state-space representation can be described as

$$\begin{bmatrix} \dot{\mathbf{x}} \\ \mathbf{z} \\ \mathbf{y} \end{bmatrix} = \begin{bmatrix} \mathbf{A}(\boldsymbol{\rho}) & \mathbf{B}_1(\boldsymbol{\rho}) & \mathbf{B}_2 \\ \mathbf{C}_1(\boldsymbol{\rho}) & \mathbf{D}_{11}(\boldsymbol{\rho}) & \mathbf{D}_{12} \\ \mathbf{C}_2 & \mathbf{D}_{21} & 0 \end{bmatrix} \begin{bmatrix} \mathbf{x} \\ \mathbf{w} \\ \mathbf{u} \end{bmatrix} \tag{1}$$

In the above equation, $\mathbf{x}$ is the state vector, $\mathbf{z}$ represents the vector of control design targets (typically specified via loop shaping) to be minimised, including performance and robustness measures, $\mathbf{y}$ stands for the measured output vector, $\mathbf{w}$ denotes the exogenous input vector, such as references (pilot commands in the aerospace applications), disturbances (wind gusts in the aerospace applications), noises, etc., $\mathbf{u}$ is the control input vector and $\boldsymbol{\rho}(t)$ is a time-varying vector of physical parameters (velocity, altitude, nacelle incidence, etc.). It is worth noting that the time variation of $\boldsymbol{\rho}(t)$ is not known in advance, but can be measured in real-time and lies in the set bounded by known minimum and maximum values.

The design objective is to find a LPV controller $\mathbf{K}(\boldsymbol{\rho})$ in the form

$$\begin{aligned} \dot{\mathbf{x}}_k &= \mathbf{A}_k(\boldsymbol{\rho})\mathbf{x}_k + \mathbf{B}_k(\boldsymbol{\rho})\mathbf{y} \\ \mathbf{u} &= \mathbf{C}_k(\boldsymbol{\rho})\mathbf{x}_k + \mathbf{D}_k(\boldsymbol{\rho})\mathbf{y} \end{aligned} \tag{2}$$

to stabilise the closed-loop interconnection shown in Fig. 1 for all admissible parameter trajectories in $\boldsymbol{\rho}(t)$, and also guarantee that the induced $\mathcal{L}_2$-norm from $\mathbf{w}$ to $\mathbf{z}$ is bounded by some $\gamma > 0$.

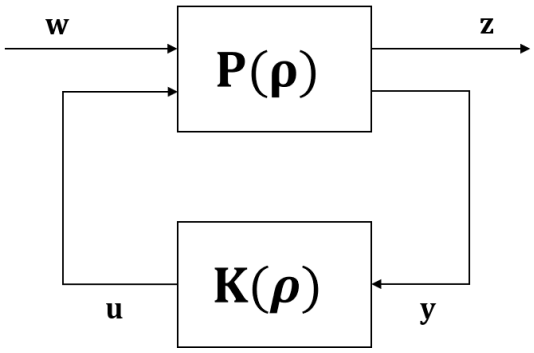

Fig. 1: Gain-scheduled $\mathcal{H}_\infty$ problem.

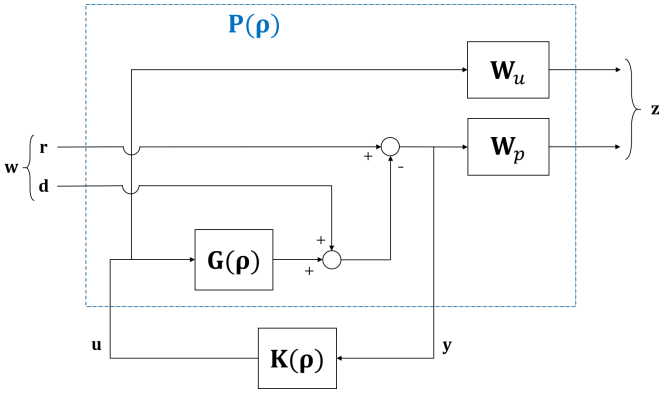

Fig. 2: Mixed-sensitivity $\mathcal{H}_\infty$ control structure.

In this work, the control synthesis used to develop $\mathbf{K}(\boldsymbol{\rho})$ solves the mixed-sensitivity optimisation criterion [23], [24]

$$\min_{\mathbf{K} \text{ stabilising}} \left\| \begin{bmatrix} \mathbf{W}_p\mathbf{S} \\ \mathbf{W}_u\mathbf{K}\mathbf{S} \end{bmatrix} \right\|_\infty \tag{3}$$

where $\mathbf{S} = (\mathbf{I} + \mathbf{G}\mathbf{K})^{-1}$ and $\mathbf{K}\mathbf{S}$ are the sensitivity and effort functions. These two transfer function establish the characteristics of the control loop according to stability, tracking, disturbance rejection characteristics and control efforts. These specifications are provided by tuning the two weights $\mathbf{W}_p$ and $\mathbf{W}_u$. Specifically, the inverse of $\mathbf{W}_p$ determines the shape of $\mathbf{S}$ and is typically selected as a low-pass filter, while the inverse of $\mathbf{W}_u$ regulates the shape of $\mathbf{K}\mathbf{S}$, which is often chosen as a high-pass filter or a constant gain. The control diagram can be described in Fig. 2, in which $\mathbf{G}(\boldsymbol{\rho})$ represents the physical plant (tilt rotor vehicle in this application), $\mathbf{r}$ and $\mathbf{d}$ are the reference and disturbance signal. Note that the generalised system $\mathbf{P}(\boldsymbol{\rho})$ can be augmented by $\mathbf{G}(\boldsymbol{\rho})$, $\mathbf{W}_u$ and $\mathbf{W}_p$, which re-captures the block diagram shown in Fig. 1.

Ultimately, a stabilising LPV controller $\mathbf{K}(\boldsymbol{\rho})$ with a minimum achievable γ can be obtained by solving a

set of LMIs provided in [19]–[21]. Such process can be efficiently executed by using the MATLAB function '*hinfgs*'.

Remark: It is highlighted that the self-scheduling $\mathcal{H}_\infty$ LPV design method is *only* suitable for affine or polytopic LPV systems [19]–[21]. However, in many aerospace applications, such as the one in this work, the physical LPV plant $\mathbf{G}(\boldsymbol{\rho})$ is constructed by assembling a set of Linear-Time-Invariant (LTI) systems, which are obtained by trimming the full nonlinear model at various flight conditions. Such LPV plants are known as grid based LPV systems [22], whose state-space matrices are nonlinearly dependent on the parameters, thus are not accepted by the LPV design approach introduced earlier. To overcome this limitation, a Higher-Order-Singular-Value-Decomposition (HOSVD) based Tensor-Product (TP) model transformation [25], [26] method is adopted. The goal of such transformation is to convert a grid based LPV system into a specific TP convex polytopic LPV model, to which the afore-mentioned LMI-based controller design tools are applicable. Compared with other LPV model conversion approaches, TP transformation is computationally less expensive and does not need problem dependent analytic derivations [25], which makes it appealing in practice. More details regarding HOSVD and TP model transformation can be found in [27] and [25], [26], respectively.

III. Flight Control System for Transition

A. Vehicle Model

This work considers a generic tilt rotor vehicle model developed by our partners at the University of Glasgow [14], whose dynamics modelling consists of the following subsystems: rotor, pylon, wing, tail plane and fuselage, see Fig. 3. Trimming of such sophisticated model exploits Automatic Differentiation (AD) method [14], which offers faster and more accurate calculation, and the results have been validated against the performance characteristics of XV-15 aircraft. More details regarding the vehicle's modelling and its validation, refer to [14], [28].

The following linearised plant is obtained by trimming the nonlinear vehicle model, which is expressed in state-space form as:

$$\begin{aligned} \dot{\mathbf{x}} &= \mathbf{A}\mathbf{x} + \mathbf{B}\mathbf{u} \\ \mathbf{y} &= \mathbf{C}\mathbf{x} + \mathbf{D}\mathbf{u} \end{aligned} \tag{4}$$

where $\mathbf{A} \in \mathbb{R}^{8\times 8}$ is the state matrix, $\mathbf{B} \in \mathbb{R}^{8\times 10}$ is the input matrix, $\mathbf{C} = \mathbf{I} \in \mathbb{R}^{8\times 8}$ is the output matrix, and

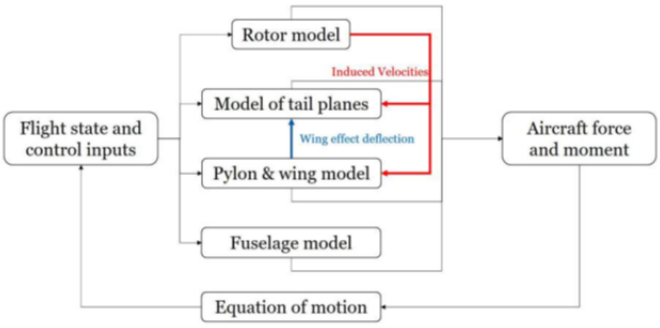

Fig. 3: Model structure.

$\mathbf{D} = 0$ is the feed-forward matrix. The state vector $\mathbf{x}$ and the input vector $\mathbf{u}$ are defined by:

$$\mathbf{x} = [u, w, q, \theta, v, p, \phi, r]^T$$
$$\mathbf{u} = [\theta_{0,C}, \theta_{lon,c}, \theta_{lat,c}, \theta_{y,c}, \delta_r, \theta_{1s,C}, \delta_e, \delta_a, \theta_{0,D}, \theta_{1s,D}]^T$$

see the Nomenclature to find a description of the above variables and their units.

During the conversion, the flight control system aims to reduce the pilots' workload and focuses on the regulation of pitch, roll and yaw motions. The corresponding control input/output pairs are: i) combined longitudinal controller ($\theta_{lon,c}$) for pitch attitude (θ) control; ii) combined lateral controller ($\theta_{lat,c}$) for roll attitude (ϕ) control; and iii) combined yawing controller ($\theta_{y,c}$) for yaw rate control. Note that the combined controllers are mixed by the swashplate and the flight control surfaces inputs. In particular, $\theta_{lon,c}$ is mixed by common collective pitch ($\theta_{1s,C}$) and elevator (δ_e), $\theta_{lat,c}$ is mixed by differential collective pitch ($\theta_{0,D}$) and aileron (δ_a), and $\theta_{y,c}$ is mixed by differential longitudinal cyclic pitch ($\theta_{1s,D}$) and rudder (δ_r). In practice, these combined controllers operate on the following principle (take the longitudinal combined controller for instance): 1 inch deflection of the combined longitudinal controller leads to a deg elevator deflection together with b deg common longitudinal cyclic deflection, where a and b change according to the nacelle incidence and flight speed, and are are set according to [28]. Mathematically, it can be described by:

$$\begin{bmatrix} \theta_{1s,C} \\ \delta_e \end{bmatrix} = \begin{bmatrix} a \\ b \end{bmatrix} \theta_{lon,c}$$

B. LPV Plant Construction

Prior to the control design, a grid based LPV plant $\mathbf{G}(\boldsymbol{\rho})$ is first established by linearising the nonlinear

Plant	$\mathbf{W}_p$	$\mathbf{W}_u$	$\mathcal{H}_\infty$ performance level (γ)
Longitudinal	$\frac{s+2}{2s+0.002}$	$\frac{s+0.03}{0.1s+3}$	2.886
Lateral	$\begin{bmatrix} \frac{s+3.2}{2s+0.0032} & \\ & \frac{s+2}{2s+0.002} \end{bmatrix}$	$\begin{bmatrix} \frac{s+0.06}{0.1s+6} & \\ & \frac{s+0.06}{0.1s+6} \end{bmatrix}$	3.790

TABLE I: Weighting functions and achieved performance level.

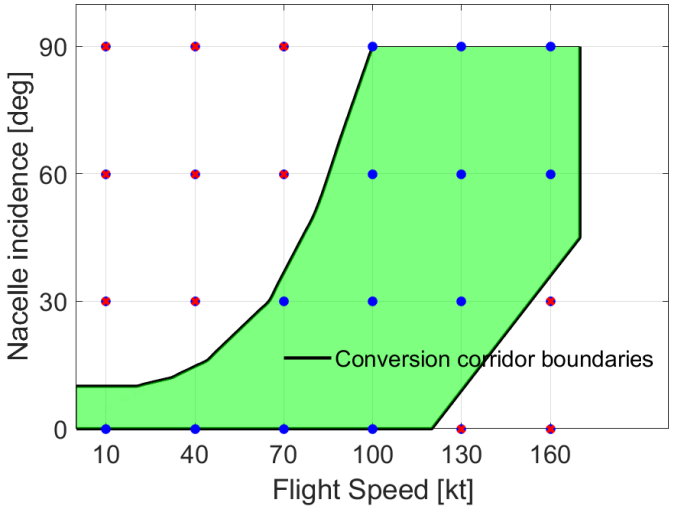

Fig. 4: Grid points of the LPV plant in transition mode.

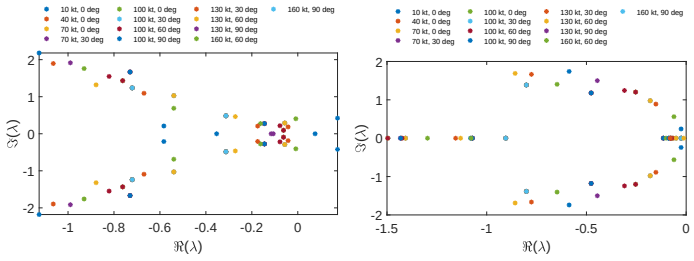

(a) (b)

Fig. 5: Poles of the grid based LPV plant. (a): longitudinal dynamics; (b): lateral dynamics.

vehicle model at a family of grid (trimming) points. The varying parameter vector is selected as

$$\boldsymbol{\rho} = [V_0, \beta_m]^T$$

where

$$V_0 \in [10, 160], \ \ \beta_m \in [0, 90]$$

and the grid density is chosen as 6×4. Typically, tighter grid density could typically lead to better control performance, while on the other hand, more computational efforts are required. Hence the trade-off between these two aspects should be considered according to the particular application. Note that $\beta_m = 0°$ indicates that the vehicle is in the helicopter configuration while $\beta_m = 90°$ implies it being fixed wing configuration.

After comparing the grid points with the XV-15 conversion corridor, we note that not all of them are within the corridor, see Fig. 4. The grid points outside the conversion corridor are marked in red, while those inside the conversion corridor are specified in blue. Because the LPV synthesis adopted in this work requires a *rectangular* parameter space, the systems at red points are replaced by the closest grid points inside the corridor, for instance, the trimmed system at 10 kt, 30 deg is replaced by the system at 10 kt, 0 deg. As long as the vehicle operates inside the conversion corridor, such replacement would not cause too much stability and performance degradation.

We then examine the poles of the grid based LPV plant, which can be observed from Fig. 5. It is clear that the vehicle is unstable at low speed conditions, helicopter configuration, while the vehicle progresses to the fixed wing configuration and high flight speed scenarios, the trimmed systems have stable poles. The migration of the poles fits the results shown in [28], [29], indicating that the grid based LPV plant provides reliable estimations of the full nonlinear model, which is fundamental for the following control design.

C. *Controller Design*

Similar to the previous work in [3], [15], a double closed-loop control structure is used, where the inner loop is known as Stability Augmentation System (SAS) and the outer controller is used for reference tracking and disturbance rejection, see Fig. 6. Examination of the open-loop plant behaviours suggests that the dynamics is largely decoupled between longitudinal and lateral axes, for this reason, the control design is performed on the

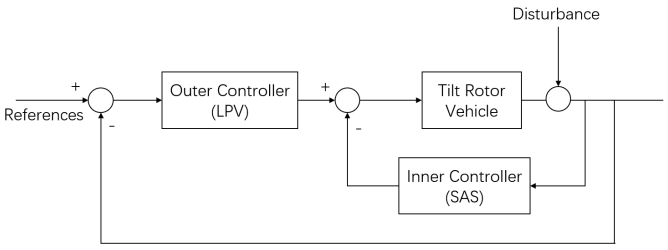

Fig. 6: Control diagram.

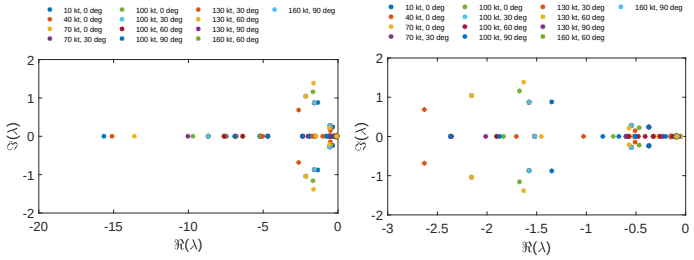

(a) (b)

Fig. 7: Poles of the inner-loop. (a): all poles; (b): zoom in.

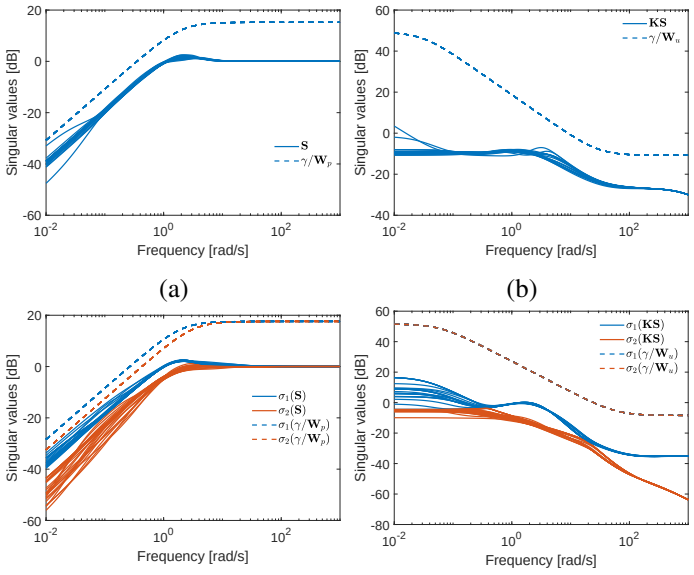

(a) (b) (c) (d)

Fig. 8: Shaped loops over the parameter space. (a) - (b): longitudinal; (c) - (d): lateral.

following two sub-models: i) longitudinal model, which consists of four states (u, w, q, θ); ii) lateral model, which is also composed of four states (v, p, ϕ, r).

The inner controller is first designed, which is hand-tuned such that it stabilises the inner-loop and enhances the time-domain performances (e.g., decreases system damping), see Fig. 7. Then the inner-loop system can be regarded as a new LPV plant, which is also grid based, and hence requires the TP model transformation introduced previously to convert it to a TP convex polytopic LPV system, suitable for the use of self-scheduling $\mathcal{H}_\infty$ design method. The weight choices for the LPV synthesis as well as the achieved $\mathcal{H}_\infty$ performance level γ are presented in Table. I. To verify that the design targets are realised, we examine the shapes of the sensitivity function and the control efforts function in Fig. 8, where the solid lines represent the shaped loops and the dashed lines are the design targets. It is clear that the singular values of $\mathbf{S}$ and $\mathbf{KS}$ are bounded by those of $\gamma/\mathbf{W}_p$ and $\gamma/\mathbf{W}_u$, respectively, i.e.,

$$\left\| \begin{bmatrix} \mathbf{W}_p\mathbf{S} \\ \mathbf{W}_u\mathbf{KS} \end{bmatrix} \right\|_\infty < \gamma \tag{5}$$

indicating that the LPV control design is successful.

IV. Simulation Results

The proposed LPV controller is examined at three frozen flight conditions as well as two conversion paths inside the conversion corridor. Detailed results are shown below.

A. Simulation at Frozen Points

The test points are chosen as: i) 50 kt, 15 deg; ii) 100 kt, 45 deg; and iii) 140 kt, 75 deg, and the following simulation focuses on the reference tracking property of the controller. The results can be seen in Fig. 9, where the references are denoted by black dashed lines. Note that the reference signal for yaw rate (r) is kept 0 during this simulation. It is clearly seen that the LPV controller provides fast tracking, negligible steady-state error and minor coupling effects between pitch, roll and yaw. Moreover, it is observed that the proposed control law is able to keep the performance level similar at all three test points, which is a preferred property in practice.

We further investigate the control actions in this simulation, which are presented in Fig. 10. It is noted that they are expressed in terms of the swashplate and flight control surface inputs, which are calculated by using the corresponding mixing algorithm in each combined controller. Clearly, they are all within reasonable ranges.

B. Simulation on Conversion Paths

We proceed to evaluate the LPV controller on two conversion paths from helicopter to fixed wing: fast and routine, see Fig. 11. In both paths, it is assumed that the

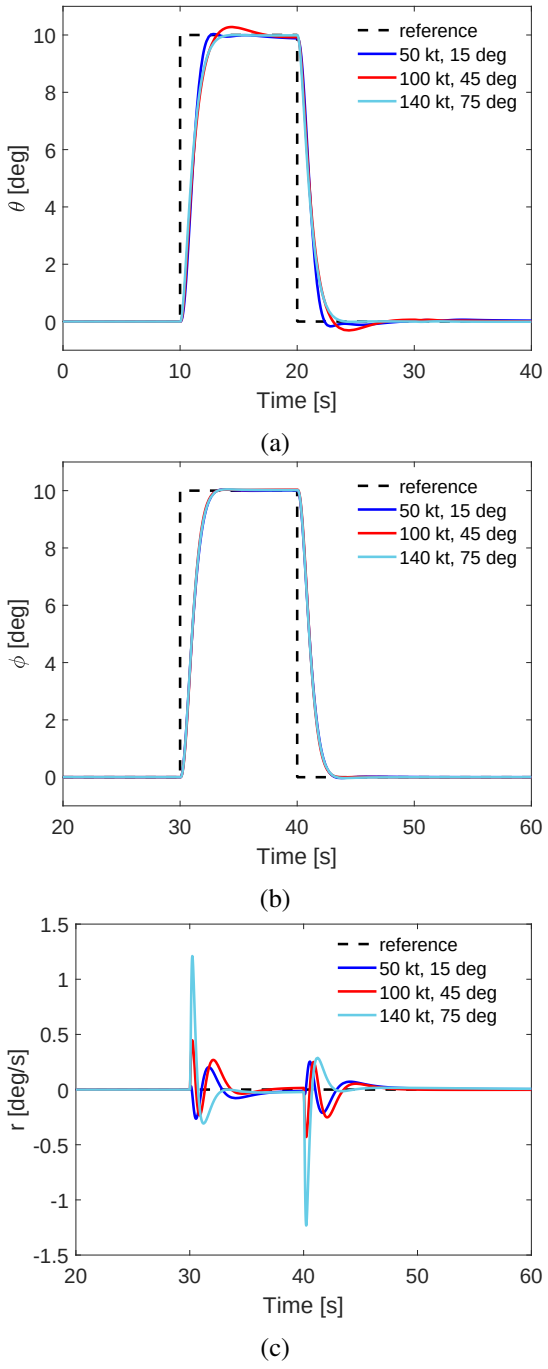

Fig. 9: Simulation results (frozen points). (a): θ; (b): ϕ; (c): r.

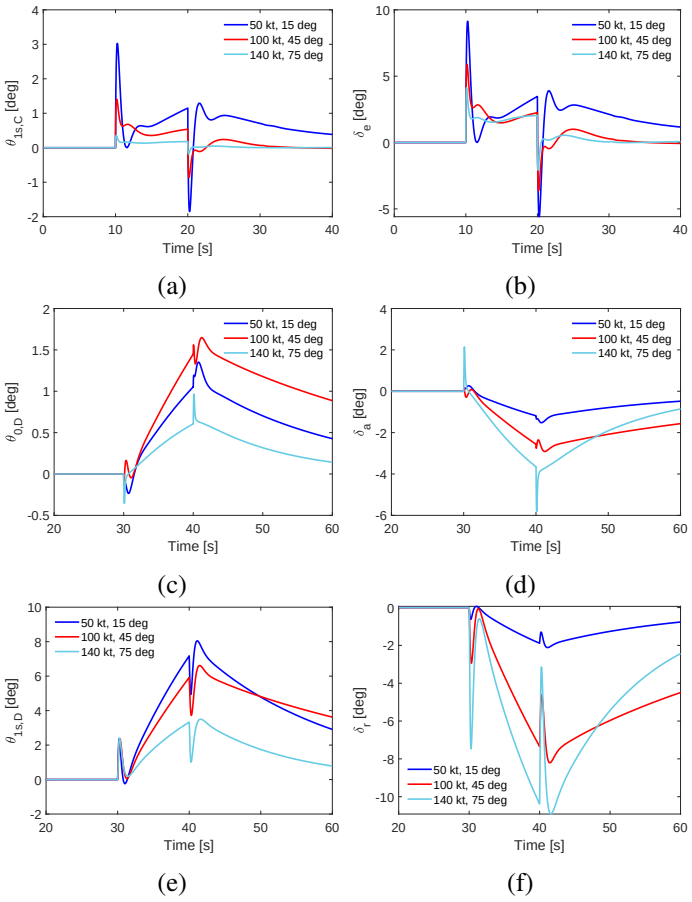

Fig. 10: Control actions (frozen points). (a): $\theta_{1s,C}$; (b): δ_e; (c): $\theta_{0,D}$; (d): δ_a; (e): $\theta_{1s,D}$; (f): δ_r.

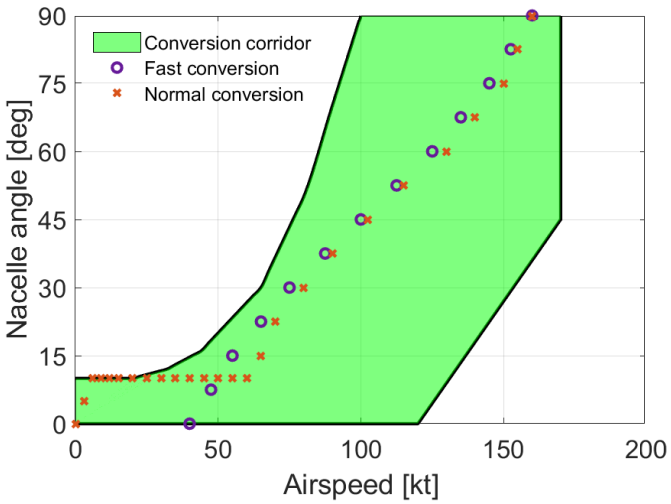

Fig. 11: Conversion paths used for the simulation.

vehicle's nacelle incidence and flight speed follow the trajectories described in Fig. 12. In particular, the fast path corresponds to the non-stop transition, which starts at 40 kt, helicopter configuration with the conversion rate being 7.5°/s, leading to a total 12 sec conversion time. The routine path represents the normal conversion typically used for XV-15, which starts at hover, helicopter configuration and takes 25 sec. It is worth noting that in this path, the transition pauses at 10 deg nacelle incidence until the vehicle reaches 70 kt flight speed.

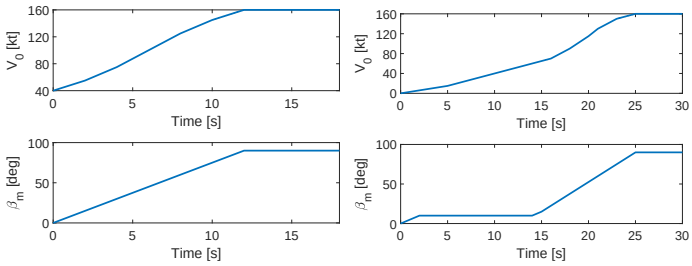

(a) (b)

Fig. 12: Flight speed and nacelle incidence trajectories. (a): fast conversion; (b): routine conversion.

In order to observe the vehicle's behaviour during transition, the simulation is currently performed on a LPV system, whose parameter space is

$$\boldsymbol{\rho} = [V_0, \beta_m]^T$$

where $V_0 \in [0, 160]$ and $\beta_m \in [0, 90]$. The grid density is chosen as 16×4, which is tighter compared with the LPV plant used for the controller design.

The simulation results can be found in Fig. 13. The disturbance signals are chosen as step signals, which are the most challenging disturbances in practice. Furthermore, they are introduced explicitly in the middle of the conversion. We observe that in both scenarios, the disturbances can be quickly attenuated by the LPV controller in all three channels (pitch, roll and yaw) within approximately 2 sec, which. This is appealing in the sense that the pilots workload can be reduced, which enhances the transition safety.

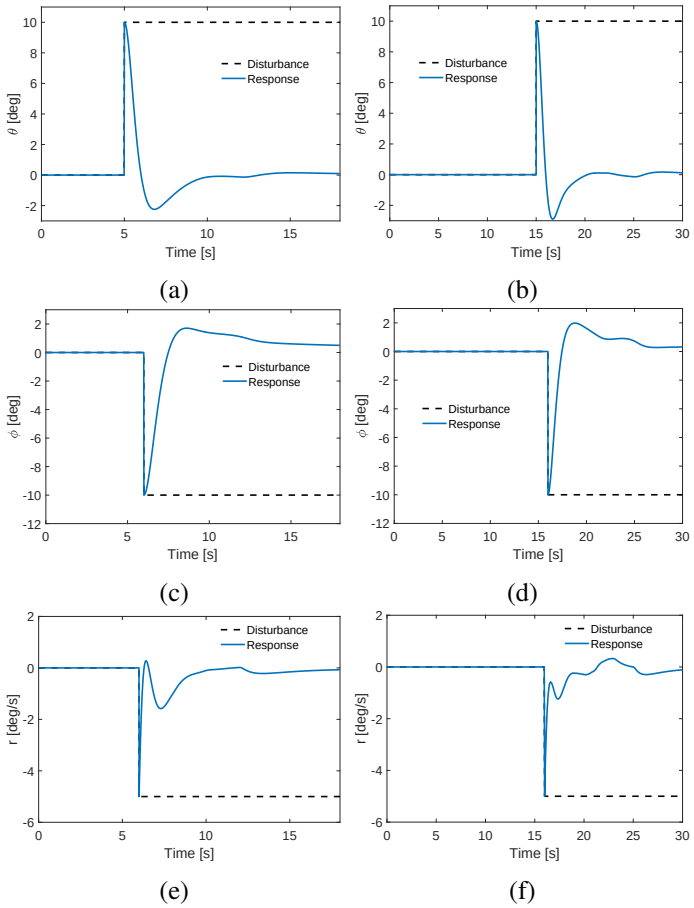

(a) (b) (c) (d) (e) (f)

Fig. 13: Simulation results (conversion paths). Left column: fast conversion; Right column: routine conversion.

V. Conclusions

This work exploits a LPV control design approach, known as self-scheduling $\mathcal{H}_\infty$, to develop the flight control system for transition. Compared with typical control methods adopted for such period, this method guarantees the closed-loop stability as well as the performance level being bounded by some prescribed value over the entire flight envelope under consideration. Linear simulation results performed on a validated XV-15 vehicle model confirm the afore-mentioned benefits, in which the proposed controller shows great performance in terms of reference tracking and disturbance rejection. Future work will implement such control method on the full nonlinear model for detailed assessment.

Acknowledgment

This work is carried out as part of the grant MENtOR (Methods and Experiment for Novel Rotorcraft, EP/S009981/1), and the authors would like to thank in EPSRC (Engineering and Physical Sciences Research Council) for their financial support. The authors are part of the UK Vertical Lift Network (UKVLN), a group of rotorcraft specialist in the UK. Authors are also grateful to the various UKVLN members for their comments and feedback on this work.

Reference

[1] H. Yang and R. Morales, "Robust full-envelope flight control design for an eVTOL vehicle," in *Proceedings of AIAA Scitech 2021 Forum*, 2021.

[2] S. Panza, L. Guastalla, B. Roda, and M. Lovera, "Tilt-rotor multivariable attitude control with rotor state feedback," *IFAC-PapersOnLine*, vol. 49, no. 17, pp. 100 – 105, 2016. 20th IFAC Symposium on Automatic Control in Aerospace (ACA) 2016.

[3] H. Yang and R. M. Morales, "Robust flight control for a validated XV-15 model," in *Proceedings of VFS Forum 77*, 2021.

[4] C. Papachristos, K. Alexis, and A. Tzes, "Design and experimental attitude control of an unmanned tilt-rotor aerial vehicle," in *2011 15th International Conference on Advanced Robotics (ICAR)*, pp. 465–470, 2011.

[5] C. Papachristos, K. Alexis, and A. Tzes, "Towards a high-end unmanned tri-tiltrotor: design, modeling and hover control," in *2012 20th Mediterranean Conference on Control Automation (MED)*, pp. 1579–1584, 2012.

[6] H. Yang and R. Morales, "Full-envelope flight control for a multi-rotor cessna-182 eVTOL," in *Proceedings of European Rotorcraft Forum 2020*, 2020.

[7] D. N. Cardoso, S. Esteban, and G. V. Raffo, "A new robust adaptive mixing control for trajectory tracking with improved forward flight of a tilt-rotor uav," *ISA Transactions*, 2020.

[8] J. Dickeson, D. Miles, O. Cifdaloz, V. Wells, and A. Rodriguez, "Robust LPV $\mathcal{H}_\infty$ gain-scheduled hover-to-cruise conversion for a tilt-wing rotorcraft in the presence of CG variations," in *Proceedings of the 46th IEEE Conference on Decision and Control 2007, CDC*, pp. 2773–2778, 2007.

[9] H. Yang and R. M. Morales, "Linear parameter varying control for XV-15 tiltrotor vehicle during transition," in *Proceedings of European Rotorcraft Forum 2021*, 2021.

[10] T. Lombaerts, J. Kaneshige, S. Schuet, B. Aponso, K. Shish, and G. Hardy, "Nonlinear dynamic inversion based attitude control for a hovering quad tiltrotor eVTOL vehicle," in *Proceedings of AIAA Scitech 2019 Forum*, 2019.

[11] T. Lombaerts, J. Kaneshige, S. Schuet, B. L. Aponso, K. H. Shish, and G. Hardy, "Dynamic inversion based full envelope flight control for an eVTOL vehicle using a unified framework," in *Proceedings of AIAA Scitech 2020 Forum*, 2020.

[12] Z. Liu, Y. He, L. Yang, and J. Han, "Control techniques of tilt rotor unmanned aerial vehicle systems: A review," *Chinese Journal of Aeronautics*, vol. 30, no. 1, pp. 135 – 148, 2017.

[13] D. J. Leith and W. E. Leithead, "Survey of gain-scheduling analysis and design," *International Journal of Control*, vol. 73, no. 11, pp. 1001–1025, 2000.

[14] Y. Yuan, D. Thomson, and D. Anderson, "Application of automatic differentiation for tilt-rotor aircraft flight dynamics analysis," *Journal of Aircraft*, pp. 1–6, 2020.

[15] H. Yang and R. M. Morales, "Flight control design for a validated XV-15 tilt rotor model: $\mathcal{H}_\infty$ vs linear parameter varying," in *Proceedings of European Control Conference 2021*, 2021.

[16] G. Balas, J. Mueller, and J. Barker, "Application of gain-scheduled, multivariable control techniques to the F/A-18 system research aircraft," in *Guidance, Navigation, and Control Conference and Exhibit*.

[17] Z. Lin, *Gain scheduling of aircraft pitch attitude and control of discrete, affine, linear parametrically varying systems*. PhD thesis, Iowa State University, 2002.

[18] G. J. Balas, I. Fialho, A. Packard, J. Renfrow, and C. Mullaney, "On the design of LPV controllers for the F-14 aircraft lateral-directional axis during powered approach," in *Proceedings of the 1997 American Control Conference*, vol. 1, pp. 123–127 vol.1, 1997.

[19] P. Apkarian, P. Gahinet, and G. Becker, "Self-scheduled $\mathcal{H}_\infty$ control of linear parameter-varying systems: a design example," *Automatica*, vol. 31, no. 9, pp. 1251–1261, 1995.

[20] G. Becker and A. Packard, "Robust performance of linear parametrically varying systems using parametrically-dependent linear feedback," *Systems & Control Letters*, vol. 23, no. 3, pp. 205–215, 1994.

[21] A. Packard, "Gain scheduling via linear fractional transformations," *Systems & Control Letters*, vol. 22, no. 2, pp. 79–92, 1994.

[22] F. Wu, *Control of Linear Parameter Varying Systems*. PhD thesis, University of California at Berkeley, 1995.

[23] D. W. Gu, P. H. Petkov, and M. M. Konstantinov, *Robust Control Design with MATLAB*. Springer, 2005.

[24] S. Skogestad and I. Postlethwaite, *Multivariable Feedback Control: Analysis and Design (Second Edition)*. John Wiley & Sons, 2005.

[25] P. Baranyi, "TP model transformation as a way to LMI-based controller design," *IEEE Transactions on Industrial Electronics*, vol. 51, no. 2, pp. 387–400, 2004.

[26] B. Takarics, A. Szöllsi, and B. Vanek, "Tensor product type polytopic LPV modeling of aeroelastic aircraft," in *2018 IEEE Aerospace Conference*, pp. 1–10, 2018.

[27] L. De Lathauwer, B. De Moor, and J. Vandewalle, "A multilinear singular value decomposition," *SIAM Journal on Matrix Analysis and Applications*, vol. 21, no. 4, pp. 1253–1278, 2000.

[28] S. W. Ferguson, "A mathematical model for real time flight simulation of a generic tilt-rotor aircraft," 1998. NASA CR-166536.

[29] M. D. Maisal, "Tilt rotor research aircraft familiarization document," 1975. Technical Report TM X-62,407, NASA.